

WPO 42488

Uranium Series Disequilibrium Investigations
Related to the WIPP Site, New Mexico

Part I

A Preliminary Study of Uranium-Thorium Systematics in Dissolution Residues
at the Top of Evaporites of the Salado Formation - Implications to Process and Time

by

B. J. Szabo, U.S. Geological Survey, Denver,
Colorado 80225

and

W. C. Gottschall, U.S. Geological Survey, Denver, Colorado 80225
and University of Denver, Denver, Colorado 80208

Part II

Uranium Trend Dating of Surficial Deposits and Gypsum Spring
Deposit Near WIPP Site, New Mexico

by

J. N. Rosholt and C. R. McKinney, U.S. Geological Survey, Denver,
Colorado 80225

Prepared by the U.S. Geological Survey
for the
Albuquerque Operations Office
U.S. Department of Energy
(Memorandum of Understanding E(29-2)-3627)

OPEN-FILE REPORT 80-879

U.S. GEOLOGICAL SURVEY
WRD. LIBRARY
P. O. BOX 25659
ALBUQUERQUE, N. M. 87125

SZABO, ET AL. 80-879

PART I

INTRODUCTION

Just how suitable salt beds are for permanent disposal of radioactive wastes has been the subject of extensive studies covering diverse aspects over the past decade. The proposed site of the Waste Isolation Pilot Plant (WIPP) is located in southeast New Mexico, about 42 km east of Carlsbad, where plans are to construct the storage facility in rock salt beds of the Permian Salado Formation. Detailed surface and subsurface geology at the site and of the surrounding area has been discussed previously (Bachman, 1976; Powers and others, 1978).

A basic concern for waste repositories in salt beds is their high solubility in ground waters. Different kinds of dissolution features are known in most evaporite basins including the Delaware Basin, the region of the proposed WIPP site. Some primary questions that can be posed are: 1. Is there active dissolution of salt at or near the site of WIPP? 2. Is the process of salt dissolution continuous or episodic? 3. If episodic, what is the correlation between time and depth? 4. When did the last salt dissolution cycle occur? 5. What is the rate of dissolution?

Rosholt and others (1966) and Rosholt (1978) demonstrated that a process of isotopic evolution of uranium and thorium occurs in most types of sediments, altered volcanic ashes and deeply buried granites provided that some ground water is allowed to migrate through the porous zones of these materials during their geologic history. Often the analyses of the isotopes of the ^{238}U - ^{234}U - ^{230}Th - ^{232}Th system yield an estimated age for the time of deposition (uranium-trend age estimate) over the range of the method from 2,000 to about 800,000 years ago (Rosholt, 1978). Accordingly, it was felt that a preliminary study of salt dissolution residue samples near the WIPP site

may yield insight into the dissolution processes and/or it may provide a uranium-trend age estimate for the most recent salt dissolution that produced clay residuum and bands of gypsum. The application of uranium trend dating in the investigation of the age of surficial deposits in the area east of Carlsbad, New Mexico, is included in Part II of this report.

EXPERIMENTAL

Samples for this study came from WIPP-25, borehole drilled on the edge of Nash Draw. Nash Draw is located a few km west of the WIPP site, a feature generally attributed to solution of underlying soluble salt beds and subsidence of the overlying rock units. The detailed geologic data of drillhole WIPP-25 is reported by Sandia Laboratories and U. S. Geological Survey (1979). Eight samples were selected for the analyses of uranium and thorium isotopes from the top of Salado salt at depth of from 179.9m to 183.1m. These samples were chosen by S. J. Lambert of Sandia Laboratories and C. L. Jones and B. J. Szabo of the U. S. Geological Survey because they seemed to represent the dissolution residues most closely associated with intact salt. The samples grade from gypsum in the top sample (179.9m) through a series of redish-brown clays with increasing amounts of gypsum with depth, to halite with stringers of polyhalite (183.1m).

All of the dissolution residues (samples A through G, Table 1) were dried at 80°C for about 12 hours, crushed to a powder and then homogenized. Samples weighing about 8 g were totally dissolved by repeated addition of concentrated HF, HNO₃ and HClO₄ mixtures and dried. The residues were dissolved in 6F HCl and spiked with standard ²³⁶U, ²²⁹Th and ²²⁸Th solution. Isotopic monitoring permitted not only quantitative determinations of % recovery but also unambiguous peak energy assignment. Sample solutions were added to a previously

prepared and conditioned Dowex 1-X8 ion exchange column in the Cl^- form. Thorium does not form stable chloride complexes and hence passes directly through while the uranium chloride complexes are absorbed. (Krauss and others, 1956). The uranium is recovered in a separate beaker via subsequent elution with very dilute HCl or water. Both nitrate and/or chloride column separations can be used to further purify either the uranium or the thorium solutions since both thorium and uranium nitrate complexes are absorbed. Repetitive column treatments result eventually in a final tiny volume of very nearly pure uranium or thorium salt. The uranium solid is dissolved in a micro-drop of HClO_4 mixed with an NH_4Cl buffer and the pH adjusted to approximately 4. This solution is then added to a specially designed teflon plating apparatus and electroplated onto a disc suitable for alpha spectrometer counting. Platinum discs are used for uranium and require roughly 30 minutes of plating at a current of 1 amp. The thorium solid is dissolved in a small volume of 0.1F HNO_3 and extracted with an equally small volume of thenoyltrifluoroacetone (TTA). This organic solution is then evaporated on the disc and the extraction procedure repeated, the disc is flame dried and then placed in the alpha spectrometer for counting.

About 50 g of the halite was dissolved in slightly acidic HNO_3 solution ($\text{pH} > 1$), then iron nitrate carrier and standard ^{236}U , ^{229}Th and ^{228}Th spike solution were added. Addition of concentrated NH_4OH to the solution coprecipitated the uranium and thorium with the iron hydroxide. The precipitate was separated by centrifugation and washed with 1:20 NH_4OH . Then the precipitate was dissolved in minimal concentrated HNO_3 and the concentration adjusted to approximately 7F to permit maximum ion exchange efficiency. A previously prepared and conditioned Dowex 1-X8 ion exchange column in the NO_3^- form selectively absorbs both uranium and thorium nitrate complexes from this matrix while most other metals pass directly through. Elution with very dilute HNO_3 or water permits recovery of the relatively impurity free solution.

This solution was evaporated to dryness and the solid dissolved in 6F HCl solution, after which the treatment was identical to that indicated above.

Discs were counted for about 10,000 counts in an Ortec alpha spectrometer.

RESULTS

Results of the analyses are presented in Table 1. Uncertainties in the ratios required for plotting are listed as 2-sigma errors. The red clays (samples B through E) have uranium concentrations of about 1 to 2 ppm, whereas the mostly gypsum samples (A and G) have much lower uranium concentrations of about 0.2 ppm. The uranium content for the salt sample is about 0.017 ppm. The $^{234}\text{U}/^{238}\text{U}$ activity ratio in the salt is about unity within the limits of experimental error, but the value for $^{230}\text{Th}/^{234}\text{U}$ of 0.16 is rather low, indicating either a recent gain of uranium or loss of ^{230}Th , the daughter element of ^{234}U , from the salt that is situated just below the solution residue unconformity. Although larger sample weights were taken to compensate for the anticipated low uranium content in the salt, less significance should be placed on these numbers which differed only little from backgrounds.

The analytical data of the solution residue samples (A through G) were treated by the uranium-trend dating technique of Rosholt (1978). The method requires plots of $^{238}\text{U}/^{232}\text{Th}$ versus $^{230}\text{Th}/^{232}\text{Th}$ and $\frac{^{238}\text{U} - ^{230}\text{Th}}{^{238}\text{U}}$ versus $\frac{^{234}\text{U} - ^{238}\text{U}}{^{238}\text{U}}$ from which the uranium-trend date may be calculated. These uranium-trend plots of the solution residue samples at WIPP-25 are presented in Figure 1. The sample points, except for sample A, yield a linear relationship on the uranium-trend plots. This linear relationship indicates that the solution residue unit between 179.9 and 183.1 m represents a salt dissolution process for which the calculated uranium-trend date of the residual matter is older than 700,000 years.

DISCUSSION

The results of this study show that the uranium trend dating technique appears to be applicable to date salt dissolution residues. The observed data scatter enable one to obtain a minimum age, in this case, for that section of the core analyzed. No present day dissolution activity is indicated in the interval sampled. Indicated stability for such a long period of time resulting from this study utilizing independent chemical methodology, is in agreement with the work of Bachman, (1974).

Dissolution activity at the upper Salado Formation was the only aspect addressed in this investigation and this event may represent the most recent dissolution. Our preliminary investigation indicates moreover, that uranium-trend dating of salt dissolution residues may yield useful data. Additional samples are being analyzed from the WIPP-25 drill hole as well as WIPP 27 to determine if depth correlates with dissolution time indicating possible cyclic occurrences.

REFERENCES

- Bachman, G. O., 1974, Geologic processes and Cenozoic history related to salt dissolution in southeastern N.M.: U.S. Geological Survey Open-File Report 74-194.
- Bachman, G. O., 1976, Cenozoic deposits of southeastern N.M. and an outline of the history of evaporite dissolution, U.S. Geological Survey Journal of Research, v. 4, no. 2, p. 135-149.
- Kraus, K. A., Moore, G. E., and Nelson, F., 1956, Anion exchange studies XXI. Thorium (IV) and uranium (IV) in hydrochloric acid, separation of thorium, protactinium and uranium, J. Am. Chem. Soc., v. 78, p. 2692-2695.
- Powers, D. W., Lambert, S. J., Shaffer, S. E., Hill, L. R., and Weart, W. D., 1978, Geological Characterizations Report, WIPP site, southeastern New Mexico: Vol. I and II, SAND 78-1596, Sandia Laboratories, Albuquerque, N.M.
- Rosholt, J. N., 1978, Uranium-trend dating of alluvial deposits, in Short Papers of the Fourth International Conference, Geochronology, Cosmochronology, Isotope Geology, 1978, R. E. Zartman, ed., Geological Survey Open-File Report 78-701, p. 360-362.
- Rosholt, J. N., Doe, B. R., and Tatsumoto, M., 1966, Evolution of the isotopic composition of uranium and thorium in soil profiles, Geol. Soc. Amer. Bull., v. 77, p. 987-1004.
- Sandia Laboratories and U.S. Geological Survey, 1979, Basic Data Report for Drillhole WIPP 25 (Waste Isolation Pilot Plant - WIPP) 26 pp with appendices.

Table 1. Analytical data of WIPP-25 borehole samples. Sample A is mainly gypsum; samples B,C,D,E and F are mainly reddish-brown clays; sample G is mainly gypsum with some clay; salt is mainly halite with some polyhalite.

Sample	Depth (m)	U (ppm)	$\frac{^{234}\text{U}}{^{238}\text{U}}$	$\frac{^{230}\text{Th}}{^{238}\text{U}}$	$\frac{^{238}\text{U}}{^{232}\text{Th}}$	$\frac{^{230}\text{Th}}{^{232}\text{Th}}$	$\frac{(^{238}\text{U}-^{230}\text{Th})}{^{238}\text{U}}$	$\frac{(^{234}\text{U}-^{238}\text{U})}{^{238}\text{U}}$
(-----activity ratios-----)								
A	179.9	0.287	0.68	1.24	5.1±0.6	6.4±0.4	-0.24±0.12	-0.32±0.05
B	180.9	2.19	1.02	.98	.81±.06	.80±.04	+ .01±.06	+ .02±.05
C	181.2	1.63	.94	1.20	.76±.06	.91±.04	- .20±.07	- .06±.05
D	181.5	1.28	1.02	1.36	.76±.06	1.03±.05	- .36±.08	+ .02±.05
E	181.8	1.68	.98	1.06	.81±.06	.86±.04	- .06±.07	- .02±.05
F	182.2	1.42	.96	1.01	.77±.03	- .01±.06	- .01±.06	- .04±.05
G	182.5	.248	.93	.95	.97±.12	.92±.05	+ .05±.09	- .06±.07
Salt	183.1	.017	1.13	.18	23.2±3.5	4.1±.3	+ .82±.07	+ .13±.10

Table 2. Description and uranium and thorium concentrations in Berino soil overlying Mescalero caliche from east face of caliche quarry. NE-1/4, SW-1/4 sec. 12, T.22S., R.31E. Hat Mesa, New Mexico, 15' quadrangle.

Sample	Depth (cm)	Horizon	Description	U		Th U
				(----ppm----)		
-----Berino soil-----						
CQS 1 B	0					
CQS 1 C		Bt	Sand, fine to medium grained, well sorted,	0.561	3.29	5.88
CQS 1 D			mostly quartz, clayey, firm. Peds	.662	3.55	5.36
CQS 1 E			blocky, angular to weakly columnar.	.580	3.63	6.27
CQS 1 F	48	Btca	sand, fine to medium grained, well sorted,	.578	3.85	6.66
CQS 1 G			mostly quartz, clayey and calcareous	.593	4.13	6.96
			rests with sharp contact on K horizon	.545	3.73	6.85
	73		Disconformity, long hiatus assumed.			
-----Mescalero caliche-----						
CQC 1 H	73	K ₂ mb	Platy, very firmly cemented. Peds platy,	.483	1.60	3.31
CQC 1 I			angular, sandy, much recementation.	.592	1.91	3.23
CQC 1 J	121				.807	.608
CQC 1 K ₁		K ₃ mb	Peds blocky, angular, very	1.90	.730	.384
CQC 1 K ₂			firmly cemented. Nodular at	2.37	.105	.045
CQC 1 L			base. Engulfs underlying	.693	1.55	2.24
CQC 1 M	223		Triassic sandstone.	1.22	2.24	1.85

600

Table 3. Uranium and thorium concentrations and Th/U ratio in gypsum spring deposit exposed in arroyo. SW-1/4, SW-1/4, sec 15, T.22S., R.30E. Nash Draw, New Mexico, 15' quadrangle. 14 km west of caliche quarry.

Sample	Depth (cm)	Description	U (-----ppm-----)	Th	Th/U
—	0-30	Sand		not sampled	
GYP-1	30-45	Gypsum,	0.150	0.417	2.7
GYP-2	45-60	well cemented,	.177	.596	3.3
GYP-3	60-75	moderately wet.	.153	.547	3.5
GYP-4	75-90	Fraction of	.310	1.11	3.58
GYP-5	90-105	clay components	.437	1.47	3.36
GYP-6	105-120	increases with	.444	1.38	3.11
GYP-7	120-135	depth.	.503	1.95	3.87

Table 4. Analytical data of surficial deposits in Nash Draw and Hat Mesa, New Mexico quadrangles.

Sample	Depth (cm)	U (ppm)	$\frac{^{234}\text{U}}{^{238}\text{U}}$	$\frac{^{230}\text{Th}}{^{238}\text{U}}$	$\frac{^{238}\text{U}}{^{232}\text{Th}}$	$\frac{^{230}\text{Th}}{^{232}\text{Th}}$	$\frac{(^{238}\text{U}-^{230}\text{Th})}{^{238}\text{U}}$	$\frac{(^{234}\text{U}-^{238}\text{U})}{^{238}\text{U}}$
(-----activity ratios-----)								
Berino Soil (figure 2)								
CQS 1 B	5	0.561	1.000	1.592	0.52±0.03	0.82±0.02	-0.59±0.07	+0.±0.03
CQS 1 C	15	.662	.993	1.572	.57±.03	.89±.03	-.57±.07	-.01±.03
CQS 1 D	30	.580	1.013	1.710	.48±.02	.83±.02	-.71±.07	+0.01±.03
CQS 1 E	45	.578	.969	1.621	.46±.02	.74±.02	-.62±.07	-.03±.03
CQS 1 F	60	.593	.928	1.555	.44±.02	.68±.02	-.56±.06	-.07±.03
CQS 1 G	70	.545	.925	1.488	.44±.02	.66±.02	-.49±.06	-.08±.03
Mescalero caliche (figure 3)								
CQC 1 H	73	.483	1.129	1.020	.92±.05	.94±.03	-.02±.04	+0.13±.04
CQC 1 I	88	.592	1.182	1.037	.94±.05	.98±.03	-.04±.04	+0.18±.04
CQC 1 J	133	.807	1.451	1.258	4.03±.21	5.07±.14	-.26±.05	+0.45±.05
CQC 1 K ₁	162	1.90	1.437	1.103	7.9±.4	8.7±.2	-.10±.05	+0.44±.05
CQC 1 K ₂	164	2.37	1.550	1.154	69.2±3.6	79.8±2.2	-.15±.05	+0.55±.05
CQC 1 L	193	.693	1.126	1.227	1.35±.07	1.66±.04	-.23±.05	+0.13±.04
CQC 1 M	223	1.22	1.065	1.081	1.64±.08	1.78±.05	-.08±.04	+0.06±.03
Gypsum spring (figure 4)								
GYP-1	30-40	.150	1.258	1.682	1.09±.06	1.84±.05	-.68±.08	+0.26±.04
GYP-2	40-50	.177	1.208	1.451	.90±.05	1.31±.04	-.45±.07	+0.21±.04
GYP-3	50-60	.153	1.257	1.556	.85±.04	1.32±.04	-.56±.08	+0.26±.04
GYP-4	60-70	.310	1.117	1.392	.85±.04	1.18±.04	-.39±.07	+0.12±.04
GYP-5	70-80	.437	1.097	1.365	.90±.05	1.23±.04	-.37±.07	+0.10±.04
GYP-6	80-90	.444	1.112	1.397	.98±.05	1.36±.04	-.40±.07	+0.11±.04
GYP-7	90-99	.503	.977	1.304	.78±.04	1.02±.03	-.30±.06	-.02±.03

14

110

Table 5. Uranium-trend ages of surficial deposits in Nash Draw and Hat Mesa, New Mexico quadrangles.

<u>Deposit</u>	<u>U-trend slope</u>	<u>x-intercept 232Th index</u>	<u>Half period of F(0) (10³ yr)</u>	<u>Age (10³ y)</u>
Berino soil	-0.533	-0.480	140	330 _± 75
Mescalero caliche				
Upper part	-2.34	+0.036	590	420 _± 60
Lower part	-.419	+0.182	370	570 _± 110
Gypsum spring	-.889	-.196	340	380 _± 60

Table 6. Apparent ages using $^{230}\text{Th}/^{234}\text{U}$ and $^{234}\text{U}/^{238}\text{U}$ ratios on fossil bones from arroyo, SW-1/4, SW-1/4, sec. 15, T.22S., R.29E, Nash Draw, New Mexico quadrangle.

<u>Sample</u>	<u>Species</u>	<u>U</u> <u>dpm</u>	<u>$\frac{^{234}\text{U}}{^{238}\text{U}}$</u>	<u>$\frac{^{230}\text{Th}}{^{234}\text{U}}$</u>	<u>Apparen</u> <u>Age (10</u>
W2 Enamel (smaller tooth)	<u>Equus scotti</u>	0.88 \pm 0.03	1.99 \pm 0.04	0.22 \pm 0.01	26 \pm
W3 Enamel (larger tooth)	<u>Equus scotti</u>	.80 \pm .03	1.97 \pm .04	.26 \pm .01	32 \pm
W4 Bone (larger tibia)	Horse	65.9 \pm 2.0	2.04 \pm .04	.43 \pm .01	60 \pm
W1 Bone (Szabo collected)	?	54.0 \pm 1.6	1.97 \pm .04	.60 \pm .02	92 \pm
W5 Bone (leg bone)	Bison	22.4 \pm .7	1.91 \pm .04	.87 \pm .03	169 \pm

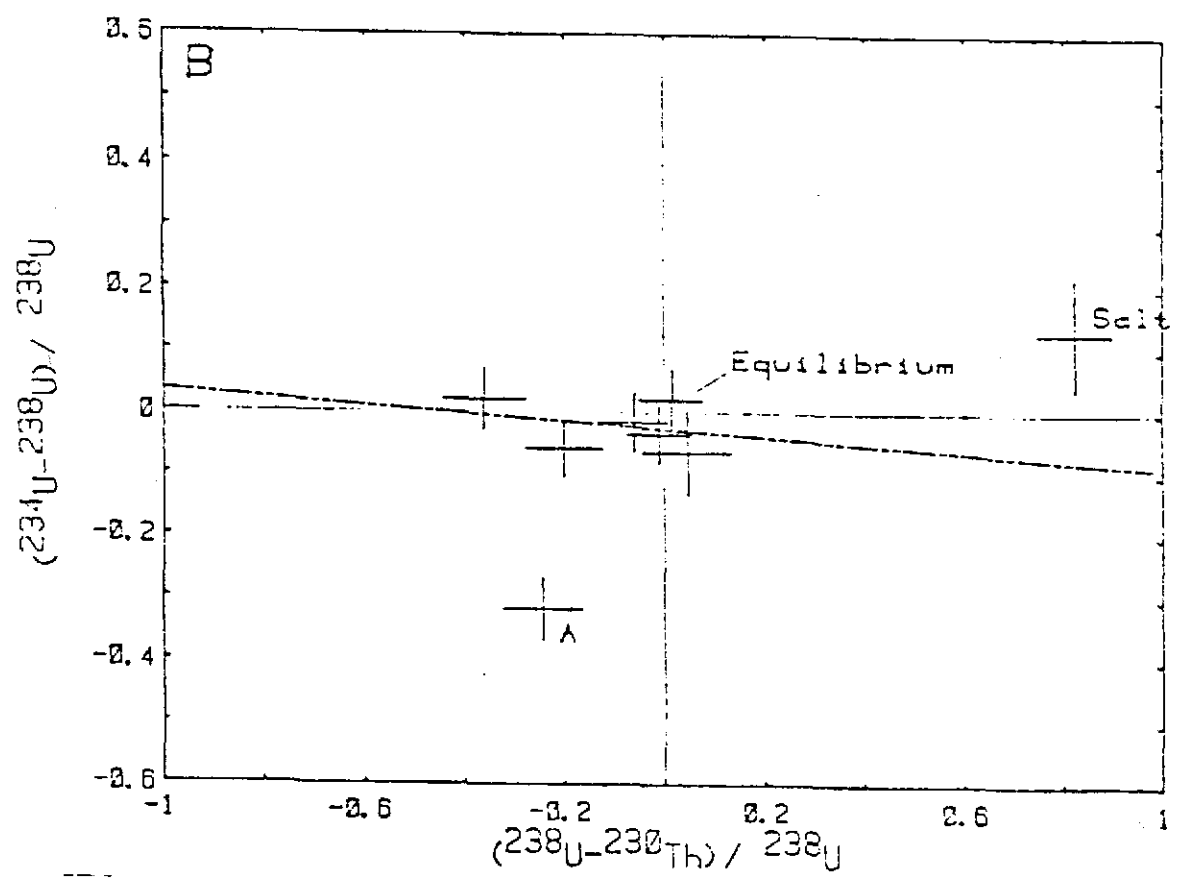
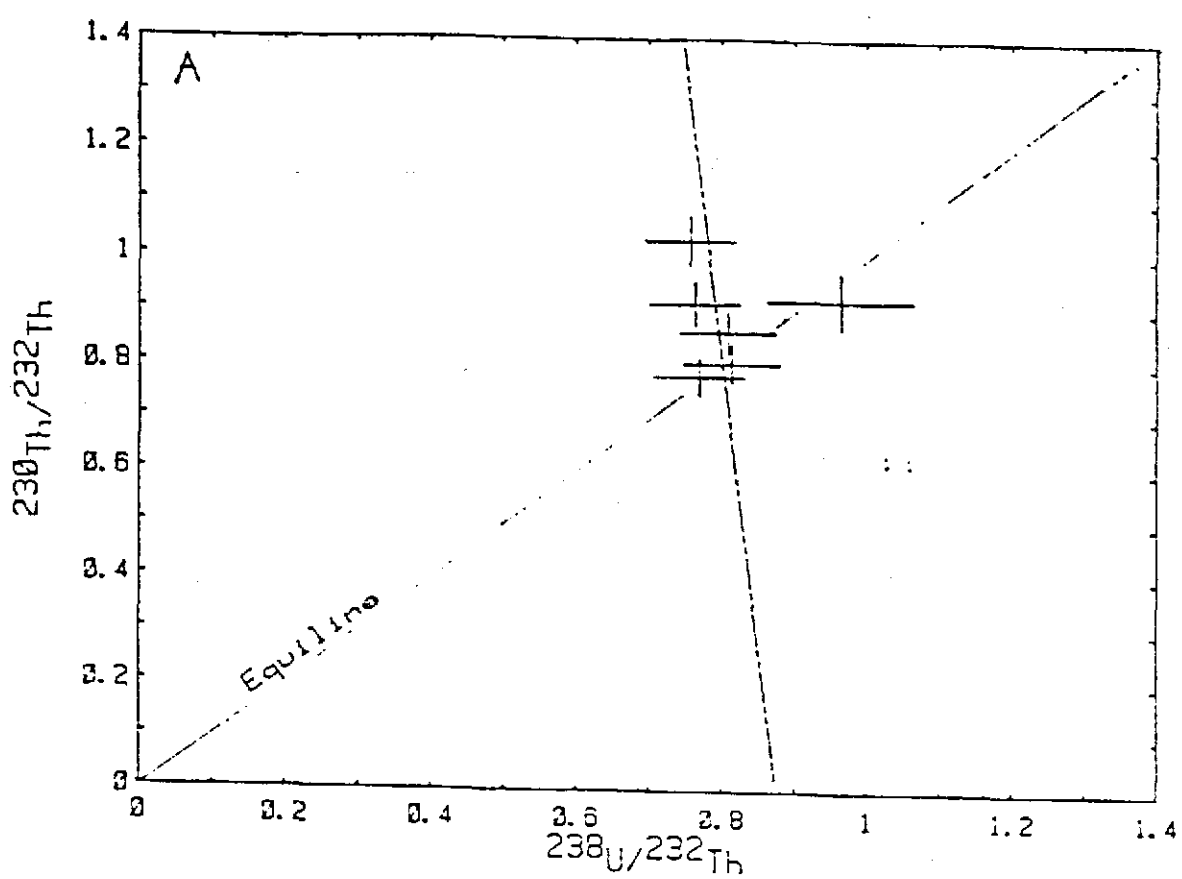


Figure 1. Uranium trend isochron plots of solution residue samples in WIPP-25 borehole. A, activity ratios, $^{238}\text{U}/^{232}\text{Th}$ versus $^{230}\text{Th}/^{232}\text{Th}$; sample A and salt are not included on plot or slope calculation. B, activity ratios, $(^{238}\text{U}-^{230}\text{Th})/^{238}\text{U}$ versus $(^{234}\text{U}-^{238}\text{U})/^{238}\text{U}$; sample A and salt are not included in slope calculation. Gypsum in sample A is interpreted to represent a previous dissolution cycle.

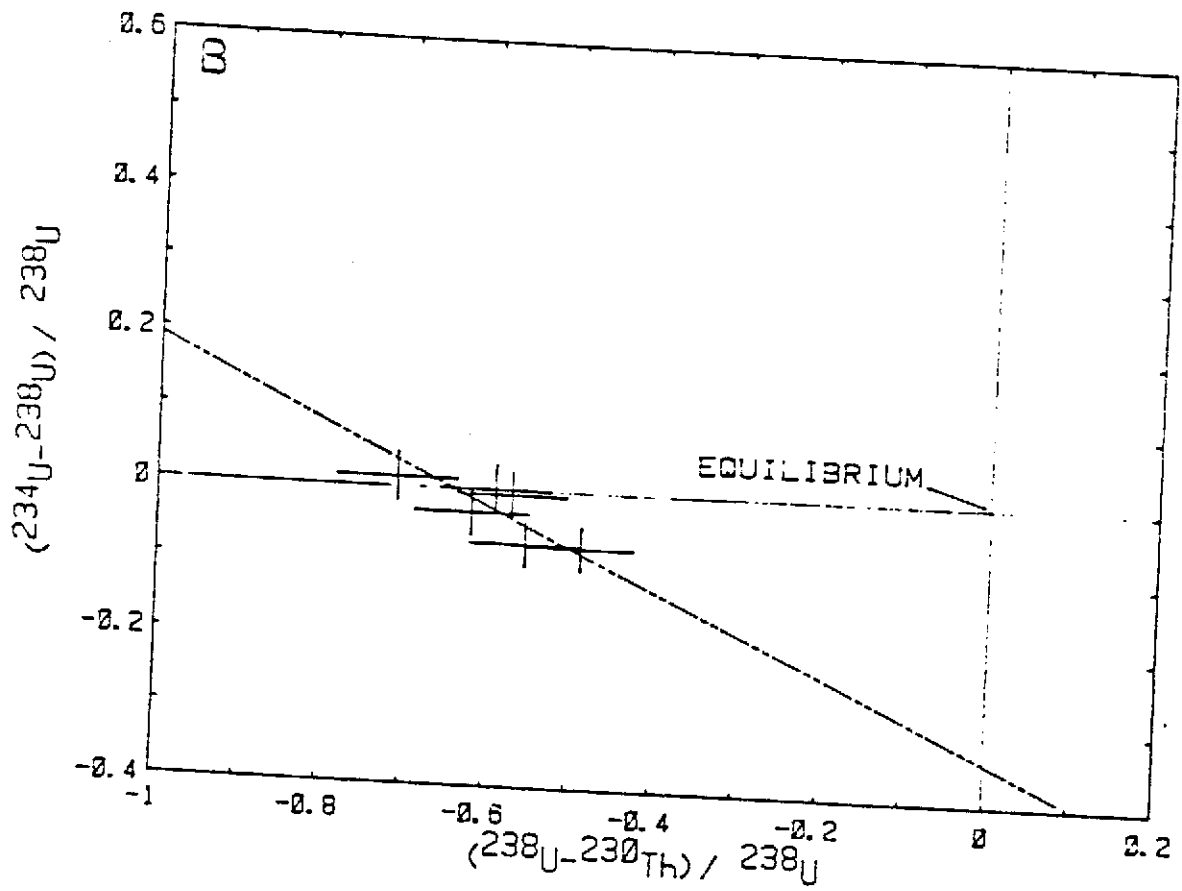
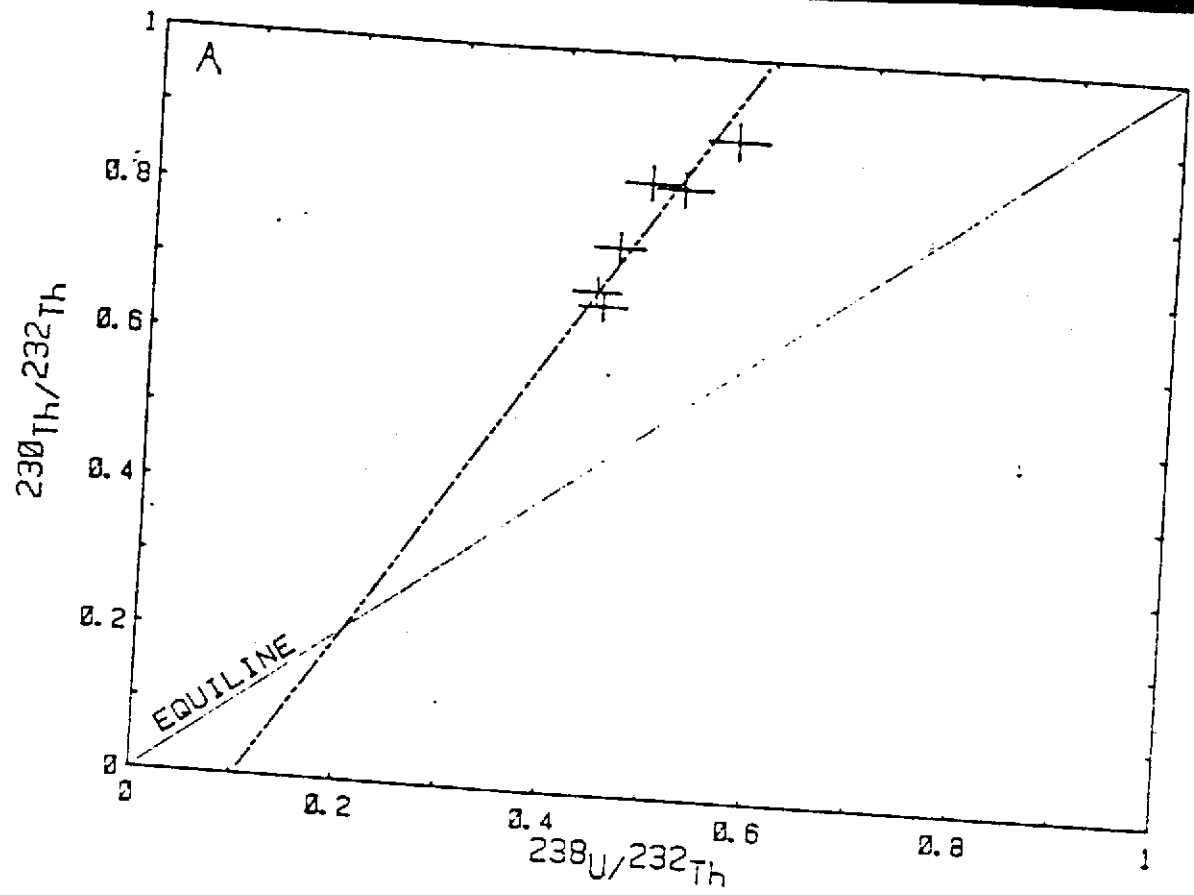


Figure 2. Uranium trend isochron plots of Berino soil section.
 A, activity ratios, $^{238}\text{U}/^{232}\text{Th}$ versus $^{230}\text{Th}/^{232}\text{Th}$.
 B, activity ratios, $(^{238}\text{U}-^{230}\text{Th})/^{238}\text{U}$ versus $(^{234}\text{U}-^{238}\text{U})/^{238}\text{U}$.

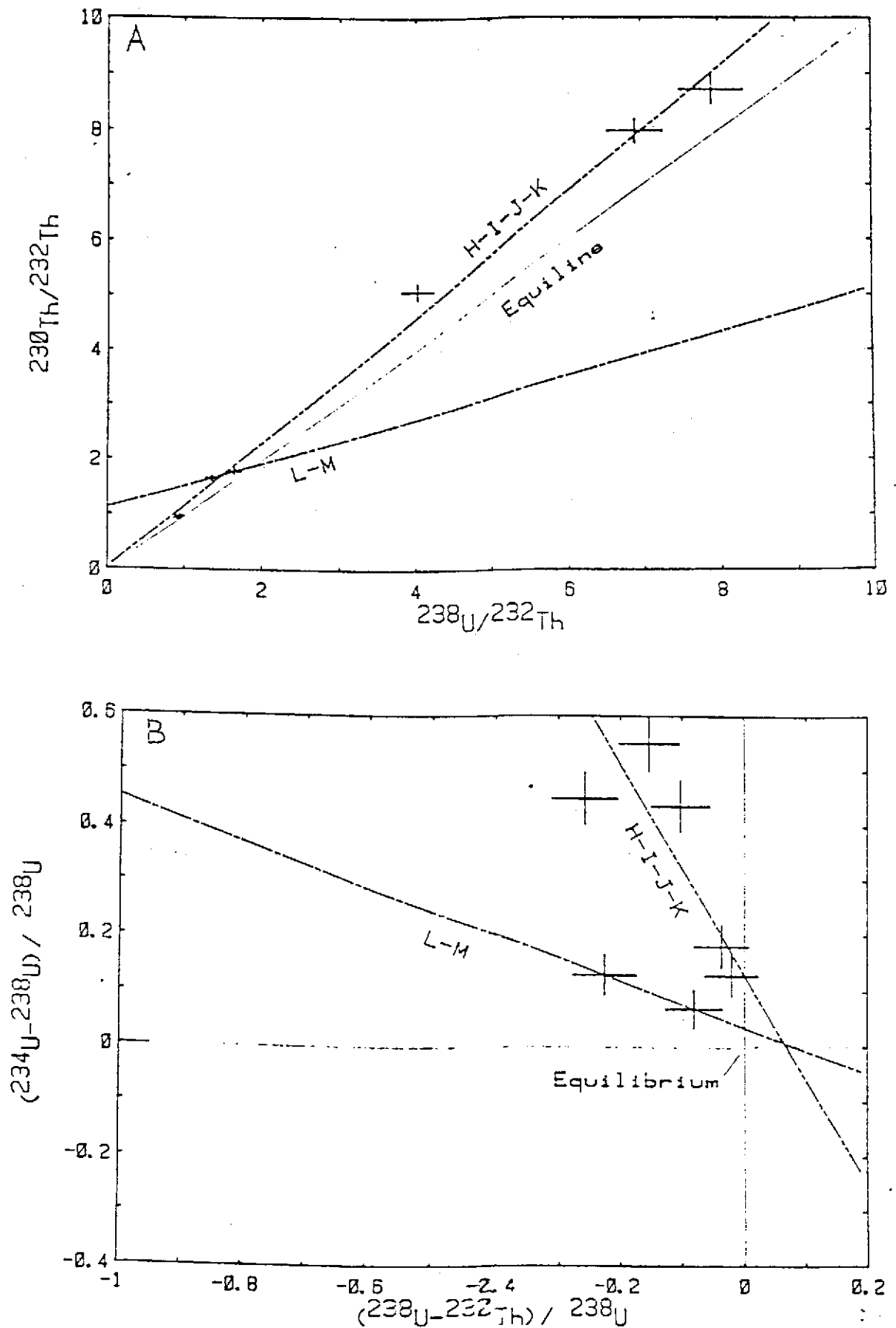


Figure 3. Uranium trend isochron plots of Mescalero caliche section.
 A, activity ratios, $^{238}\text{U}/^{232}\text{Th}$ versus $^{230}\text{Th}/^{232}\text{Th}$.
 B, activity ratios, $(^{238}\text{U}-^{230}\text{Th})/^{238}\text{U}$ versus $(^{234}\text{U}-^{238}\text{U})/^{238}\text{U}$.
 Five samples in the upper part of caliche section (H, I, J, K₁, K₂) are interpreted to represent a different age of caliche forma-

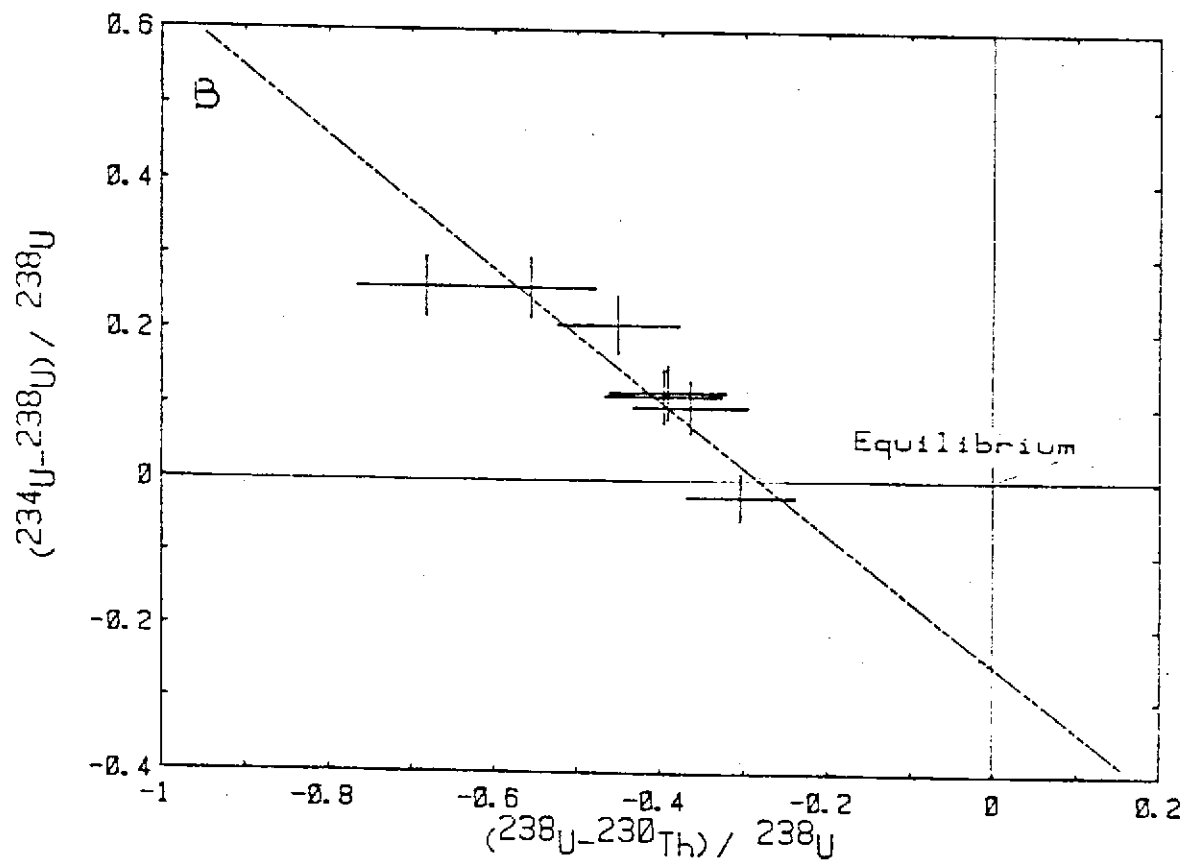
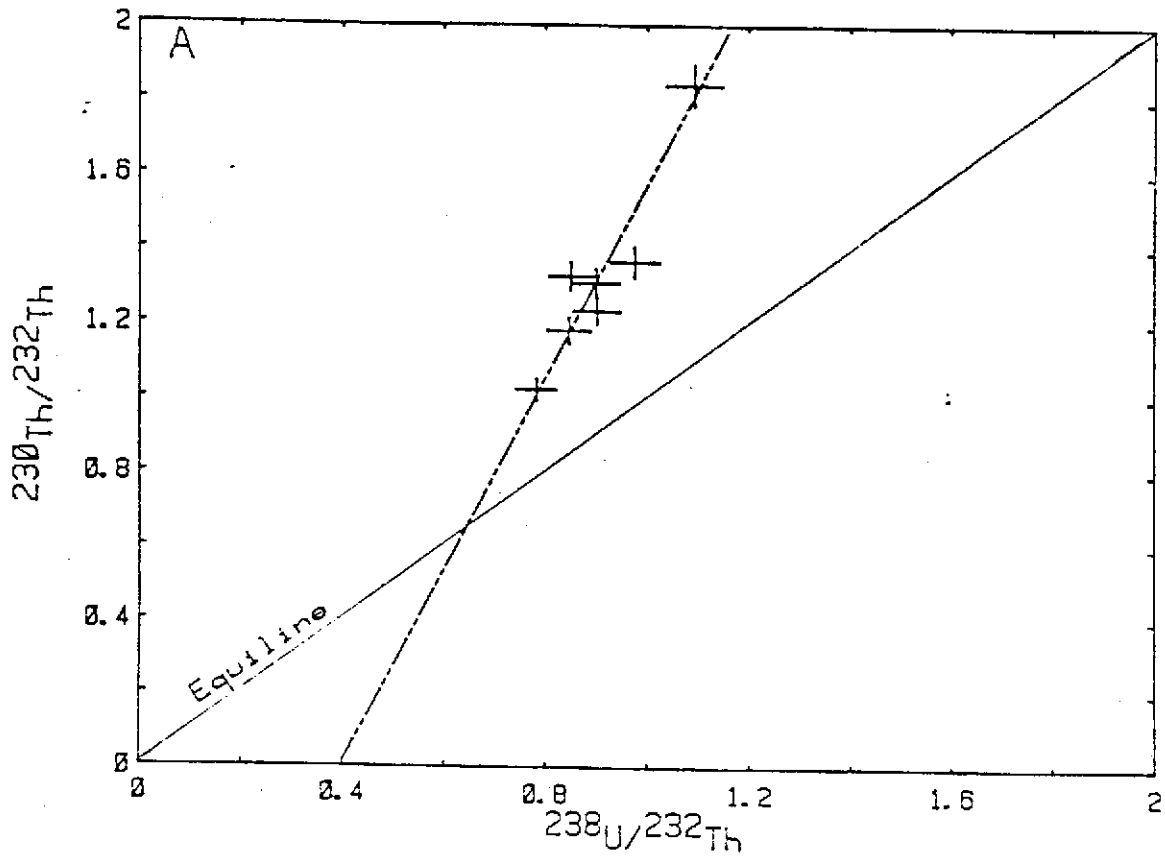


Figure 4. Uranium trend isochron plots of gypsum spring section.
 A, activity ratios, $^{238}\text{U}/^{232}\text{Th}$ versus $^{230}\text{Th}/^{232}\text{Th}$.
 B, activity ratios, $(^{238}\text{U}-^{230}\text{Th})/^{238}\text{U}$ versus $(^{234}\text{U}-^{238}\text{U})/^{238}\text{U}$.

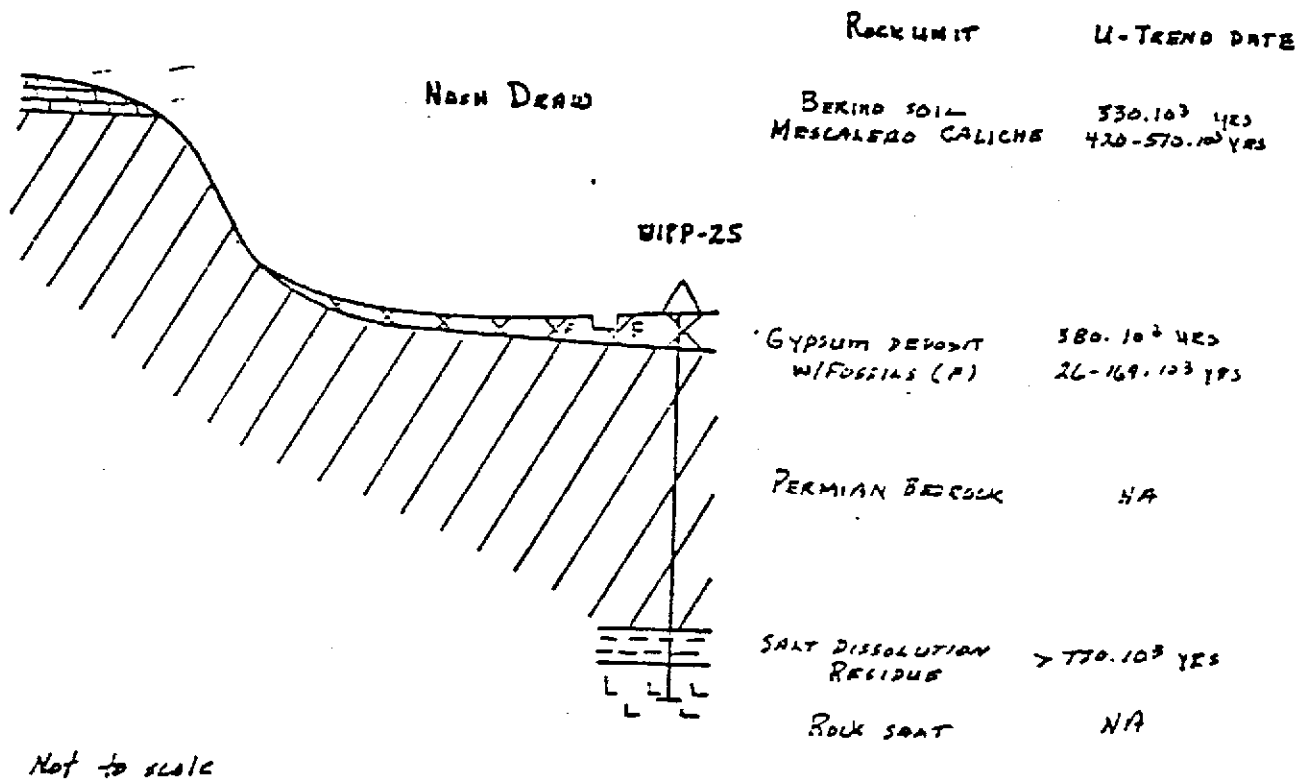


Figure 5. Spatial relations of Berino soil, Mescalero caliche, gypsum spring deposit, salt dissolution residue and rock salt. (Illustration provided by C. L. Jones.)

PART II

INTRODUCTION

Uranium-trend dating of sediments and geochemical replacement deposits is a modified version of traditional uranium-series dating. It is different than traditional $^{230}\text{Th}/^{234}\text{U}$, $^{234}\text{U}/^{238}\text{U}$, and $^{231}\text{Pa}/^{235}\text{U}$ dating that requires a closed system to satisfy rigorous mathematical solutions for calculation of reliable ages in suitable types of geological material (Ku, 1976). Because of the large number of geochemical variables associated with uranium migration in sediments, the model is based on the assumption of an open system regarding migration of uranium and some daughter products. To accommodate such open system conditions, an empirical model that requires time calibration points is used to obtain solution for ages of deposition in a variety of different types of deposits that appear to be applicable to this method of dating.

Most sediments and geochemical deposits have been subjected to interactions with the hydrologic regime associated with the sedimentary environment. Water that permeates these kinds of sedimentary deposits usually contains at least small amounts of uranium. This water-soluble uranium, upon radioactive decay, produced some radioactive daughter products that were readily adsorbed on the solid sedimentary matrix material. These trails of daughter products, especially ^{234}U and ^{230}Th , commonly were distributed in a predictable pattern in the host sediments and this pattern is the basis for the empirical uranium-trend model. A more detailed description of the empirical model has been reported (Rosholt, 1978).

Analyses on a number of alluvial and eolian deposits have been used to formulate the model and those depositional units with sufficient age control were used for time calibration points. The same empirical model is used for dating the dissolution residues in Part I and the surficial deposits in Part II.

SAMPLING REQUIREMENTS AND DEPOSIT DESCRIPTIONS

The dating technique consists of determining an isochron from analyses of several different samples representing a given depositional unit; from three to ten samples in each unit are analyzed. In each sample an accurate determination of the abundances of ^{238}U , ^{234}U , ^{230}Th , and ^{232}Th is required. Chemical procedures used to obtain the analyses are similar to those described in Part I. The results of these analyses are plotted where $(^{238}\text{U}-^{230}\text{Th})/^{238}\text{U}$ versus $(^{234}\text{U}-^{238}\text{U})/^{238}\text{U}$ ideally yields a linear relationship in which the measured slope changes in a predictable way with the increasing age of the depositional unit. Least squares fitting of a straight line to the data array using the York-fit method was used to obtain isochrons (Ludwig, 1979).

The time of deposition of three different units in the area approximately 33-47 kilometers east of Carlsbad, New Mexico, was determined by the uranium-trend technique. A description of the section of Mescalero caliche and the overlying Berino soil from the caliche quarry, collected and described by George Bachman (USGS), is shown in Table 2. Samples from thick gypsum spring exposed in an arroyo in Nash Draw were collected with George Bachman and John Hawley (New Mexico Bureau of Mines and Mineral Resources). A description

of this unit and the uranium and thorium content in samples collected is shown in Table 3.

RESULTS

Isotopic ratio analyses required for the three units and the ratios showing variation from radioactive equilibrium, required for U-trend plots, are listed in Table 4. The uncertainties in these ratios are 2-sigma errors as required by the least squares fitting of a straight line using the York-fit method (Ludwig, 1979) to obtain the isochrons shown in Figures 2, 3, and 4. The uranium-trend plots for the Berino soil, Mescalero caliche, and gypsum spring deposit, respectively, are shown in these figures.

The parameters determined from the U-trend plots and the ages of deposition of the units are listed in Table 5. These results indicate that formation of the Mescalero caliche began about 500,000 years ago and continued over a relatively long period of time and probably ceased before about 330,000 years ago when the overlying sand was deposited on which the Berino soil developed. Formation of the gypsum spring deposit appears to have begun about the time when the Mescalero caliche ceased development and its source may be related to post-Mescalero collapse. (Fig. 5) Bachman (1976, p.146) suggested that solution of evaporite and collapse of the surface occurred both before and after the accumulation of the Mescalero caliche in Nash Draw.

Five fossil bones and teeth of horse and bison were collected by Curtis McKinney from the bottom of the arroyo in which the gypsum spring was exposed. These specimens yield apparent uranium-series ages that had a considerable spread in time (Table 6). Apparent ages ranged continuously from about 25,000 years for tooth enamel to

about 170,000 years for bison leg bone. The reason for the large divergence in these apparent ages may be the result of the geochemical environment to which these bones have been subjected. The three bone samples (60,000 - 170,000 years apparent ages) have uranium contents (Table 6) that significantly decrease with increase of apparent age suggesting the possibility of late uranium addition of the fossil bone material resulting in apparent ages that may be too young. The reliability of U-series dating of fossil material influenced by a high sulfate environment, as occurs in a gypsum spring, has never been tested.

One of the best studies of U-series dating of buried fossils was done by Hansen and Begg (1970) in which they dated fossils that occurred in more favorable environments for bone preservation. They calculated an average age of $103,000 \pm 6,000$ years for four fossil specimens from the Teichert site, Sacramento area, California. The alluvium at this site has now been assigned to the middle unit of the Riverbank Formation (D. E. Marchand, 1980, oral commun.) and the best current estimate for the age of middle Riverbank alluvium is about 250,000 years (Marchant and Allwardt, 1977). Thus, it should be considered that the oldest bone dates shown in Table 6 may represent a minimum age for the start of the gypsum spring deposit in Nash Draw.

REFERENCES

- Bachman, G. O., 1976, Cenozoic deposits of southeastern N.M. and an outline of the history of evaporite dissolution, U.S. Geological Survey Journal of Research, v. 4, no. 2, p. 135-149.
- Hansen, R. O., and Begg, E. L., 1970, Age of Quaternary sediments and soils in the Sacramento area, California, by uranium and actinium series dating of vertebrate fossils: Earth and Planetary Science Letters, v. 8, p. 411-419.
- Ku, T. L., 1976, The uranium-series methods of age determination: Annual Rev. Earth and Planetary Sci. Letters, v. 4, p. 347-379.
- Ludwig, K. R., 1979, A program in Hewlett-Packard BASIC for X-Y plotting and line-fitting of isotopic and other data: U.S. Geological Survey Open-File Report 79-1641, 28 p.
- Marchand, D. E., and Allwardt, A., 1977, Late Cenozoic stratigraphic units, northeastern San Joaquin Valley, California: U.S. Geological Survey Open-File Report 77-743, 136 p.
- Rosholt, J. N., 1978, Uranium-trend dating of alluvial deposits in Short Papers of the Fourth International Conference, Geochronology, Cosmochronology, Isotope Geology, 1978, R. E. Zartman, ed., Geological Survey Open-File Report 78-701, p. 360-362.